

# Ecosystem carbon balance in the Hawaiian Islands under different scenarios of future climate and land use change

## Supplementary Material

**Authors:** Paul C. Selman<sup>1</sup>, Benjamin M. Sleeter<sup>2</sup>, Jinxun Liu<sup>1</sup>, Tamara S. Wilson<sup>1</sup>, Clay Trauernicht<sup>3</sup>, Abby G. Frazier<sup>4,5</sup>, Gregory P. Asner<sup>6</sup>

**Affiliations:**

<sup>1</sup>U.S. Geological Survey, Moffett Field, CA, USA

<sup>2</sup>U.S. Geological Survey, Seattle, WA, USA

<sup>3</sup>University of Hawai‘i at Mānoa, Honolulu, HI, USA

<sup>4</sup>East-West Center, Honolulu, HI, USA

<sup>5</sup>Clark University, Worcester, MA, USA

<sup>6</sup>Arizona State University, Tempe, AZ, USA

**Running title:** Hawai‘i carbon balance

**Keywords:** land use, climate change, carbon balance, Hawai‘i, scenarios, disturbance, ecosystem model

**Date:** August 12, 2021

## Supplementary Methods

### Moisture Zones

Agriculture, Forest, Grassland, Shrubland, and Tree Plantation land cover classes were stratified into three Moisture Zones - Dry, Mesic, and Wet (supplemental figure 1). These three zones were based on a moisture availability index (MAI), calculated as mean annual precipitation (MAP) minus potential evapotranspiration (PET; Price *et al* 2012). Areas where MAI values were less than zero (i.e.,  $MAP < PET$ ) were classified in the Dry Moisture Zone. Areas with MAI values between zero and 1,661 were classified in the Mesic Moisture Zone. The MAI value of 1,661 is roughly equivalent to areas at 1,000 m elevation that receive 2,500 mm of annual rainfall (Price *et al* 2012). Areas with MAI values greater than 1,661 were classified in the Wet Moisture Zone.

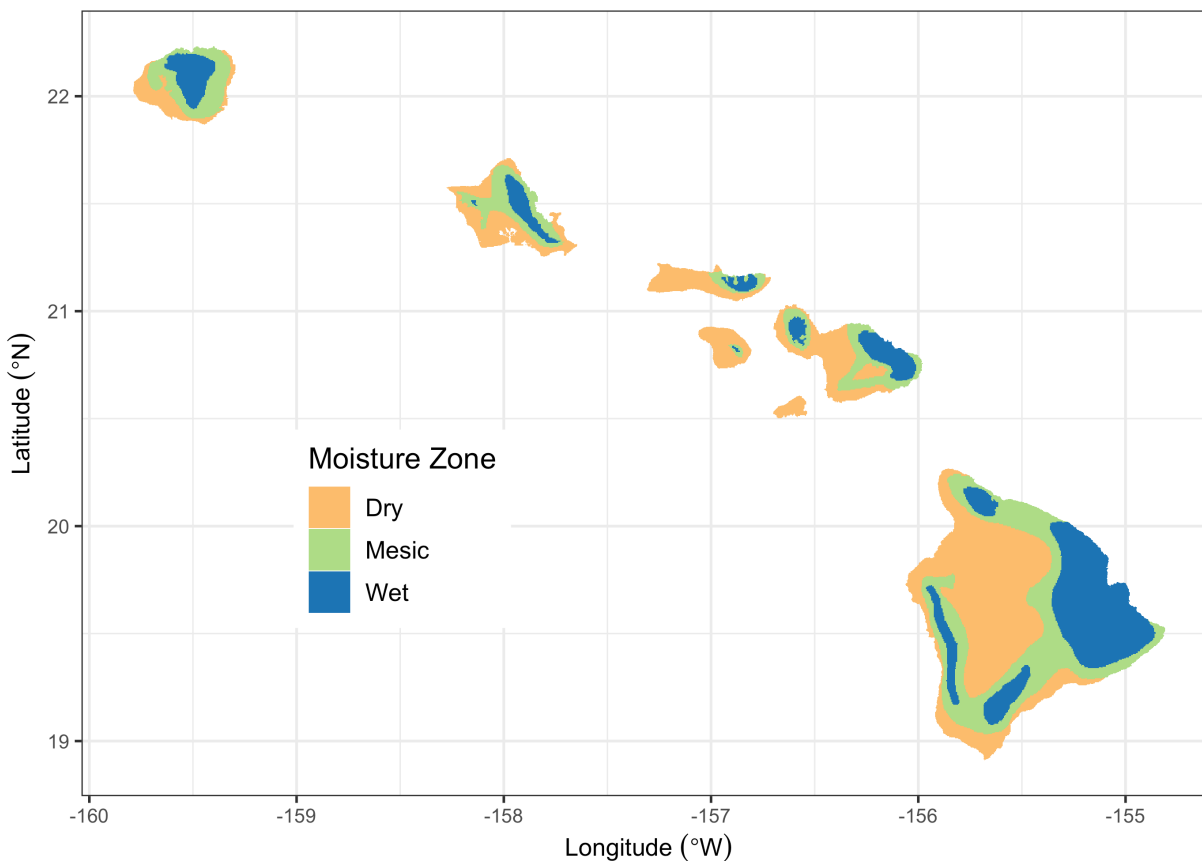


Figure 1: Supplemental - Moisture zones of the seven main Hawaiian Islands, adapted from Jacobi *et al.* (2017).

29 We used a new spatial database of wildland fire perimeters on the main Hawaiian Islands from  
 30 1999-2019 to calculate annual area burned (supplemental figure 2), wildland fire probabilities by  
 31 state type, and wildland fire size distributions. This new database compiles prior mapping efforts and  
 32 data collections with new fire perimeter data mapped by Dr. Clay Trauernicht (Department of Natural  
 33 Resources and Environmental Management, University of Hawai‘i at Mānoa). The goal was to locate  
 34 and map all fires greater than or equal to 20 hectares, but some smaller fires were included as  
 35 detected in imagery. Fire perimeters for the years 2002-2011 were primarily from the U.S. Geological  
 36 Survey Monitoring Trends in Burn Severity (MTBS; <https://www.mtbs.gov>). The Hawaii Wildfire  
 37 Management Organization ([www.hawaiiwildfire.org](http://www.hawaiiwildfire.org)) provided ground-based, GPS-mapped fire  
 38 perimeters from Hawai‘i Island, mostly from the Kona and Kohala regions. The U.S. National Park  
 39 Service provided ground-based, GPS-mapped fire records from Hawai‘i Volcanoes National Park,  
 40 and the O‘ahu Army Natural Resource Program provided ground-based, GPS-mapped fire records on  
 41 O‘ahu. All other fires were mapped directly by Dr. Trauernicht using LANDSAT and Sentinel-2  
 42 satellite imagery. Data from USGS MTBS were prioritized for the years 2002-2011 in the case of  
 43 duplicate records.

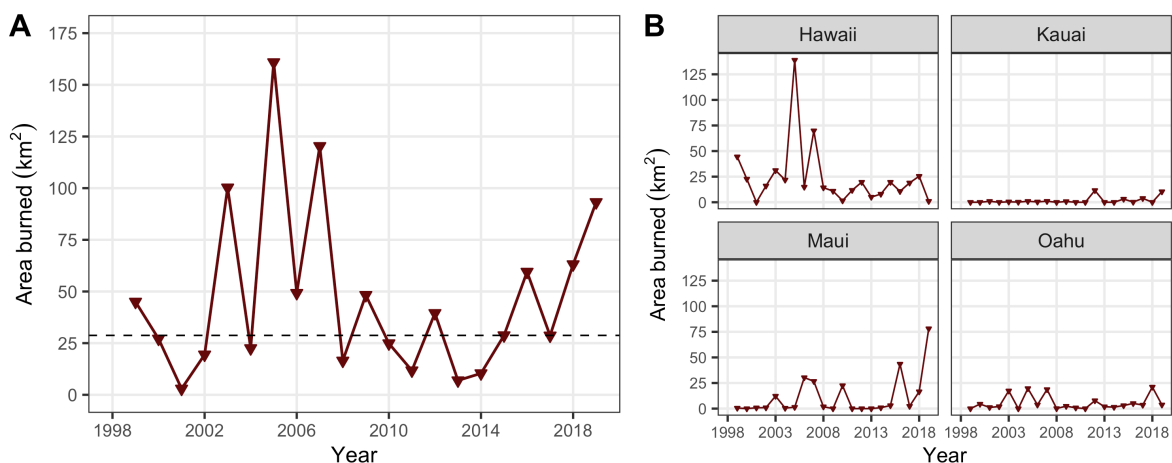


Figure 2: Supplemental - Annual area burned by wildland fire in the State of Hawai‘i from 1999-2019, summed by year across the seven main Hawaiian Islands (A) and within each of the four largest islands (B). The dashed horizontal line in (A) represents the median area burned from 1999-2019.

#### Climate

Spatially explicit contemporary mean annual temperature and rainfall data for the main Hawaiian Islands at 250-m resolution (supplemental figure 3) are from Giambelluca *et al* (2013) and Giambelluca *et al* (2014). Spatially explicit mid-century (2049-2069) and end of century (2070-2099) projections of change in annual temperature and annual rainfall (supplemental figure 4) are from statistically downscaled CMIP5 climate projections under RCP 4.5 and RCP 8.5 (Elison Timm *et al* 2015, Elison Timm 2017). To avoid biases, the modeled present-day (1975–2005) CMIP5 climatology was used to standardize the resulting predictor time series, and the simulated future changes were measured relative to their present-day mean states. See Elison Timm *et al* (2015) and Elison Timm (2017) for a more detailed description of potential statistical downscaling biases.

#### Scaling NPP

Initial values for net primary production (NPP) in LUCAS were calculated using values from the Integrated Biosphere Simulator (IBIS; supplemental table 1) adjusted with spatially explicit stationary NPP multipliers to reflect local variation driven by microclimate (supplemental Figure 5, top panel). The resulting NPP estimates (supplemental figure 5, bottom panel) preserve the IBIS-derived means for each combination of land cover class and moisture zone (supplemental table 1; Sleeter *et al* 2018, 2019). We derived the set of NPP stationary spatial multipliers by first calculating NPP independently of the IBIS values for each simulation cell using empirical relationships between annual NPP and mean annual rainfall or temperature (Schuur 2003, Del Grosso *et al* 2008) based on Hawai‘i-specific contemporary climate data (supplemental Figure 3; Giambelluca *et al* (2013); Giambelluca *et al* (2014)). We then calculated the NPP spatial multipliers as the NPP anomaly for each simulation cell relative to the mean of these empirically-derived NPP values for each unique combination of moisture zone and land cover class (supplemental Figure 5, top panel). LUCAS model NPP was initiated using the product of stationary spatial NPP multipliers (supplemental figure 5, top panel) and IBIS-derived NPP (supplemental table 1).

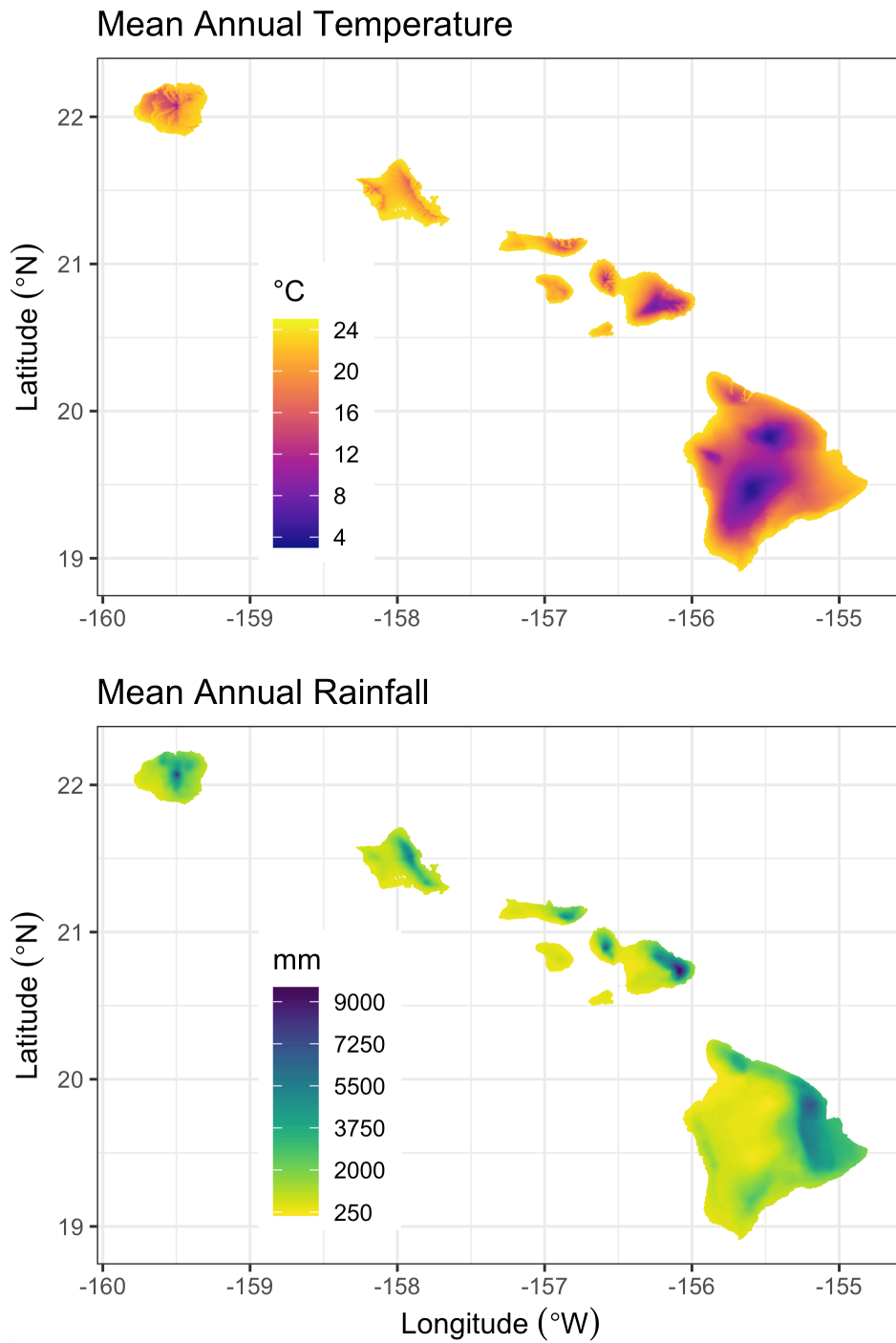


Figure 3: Supplemental - Contemporary 30-year climate normals for mean annual temperature (top panel) and mean annual rainfall (bottom panel) for the seven main Hawaiian Islands. Data from Giambelluca *et al.* (2013) and Giambelluca *et al.* (2014).

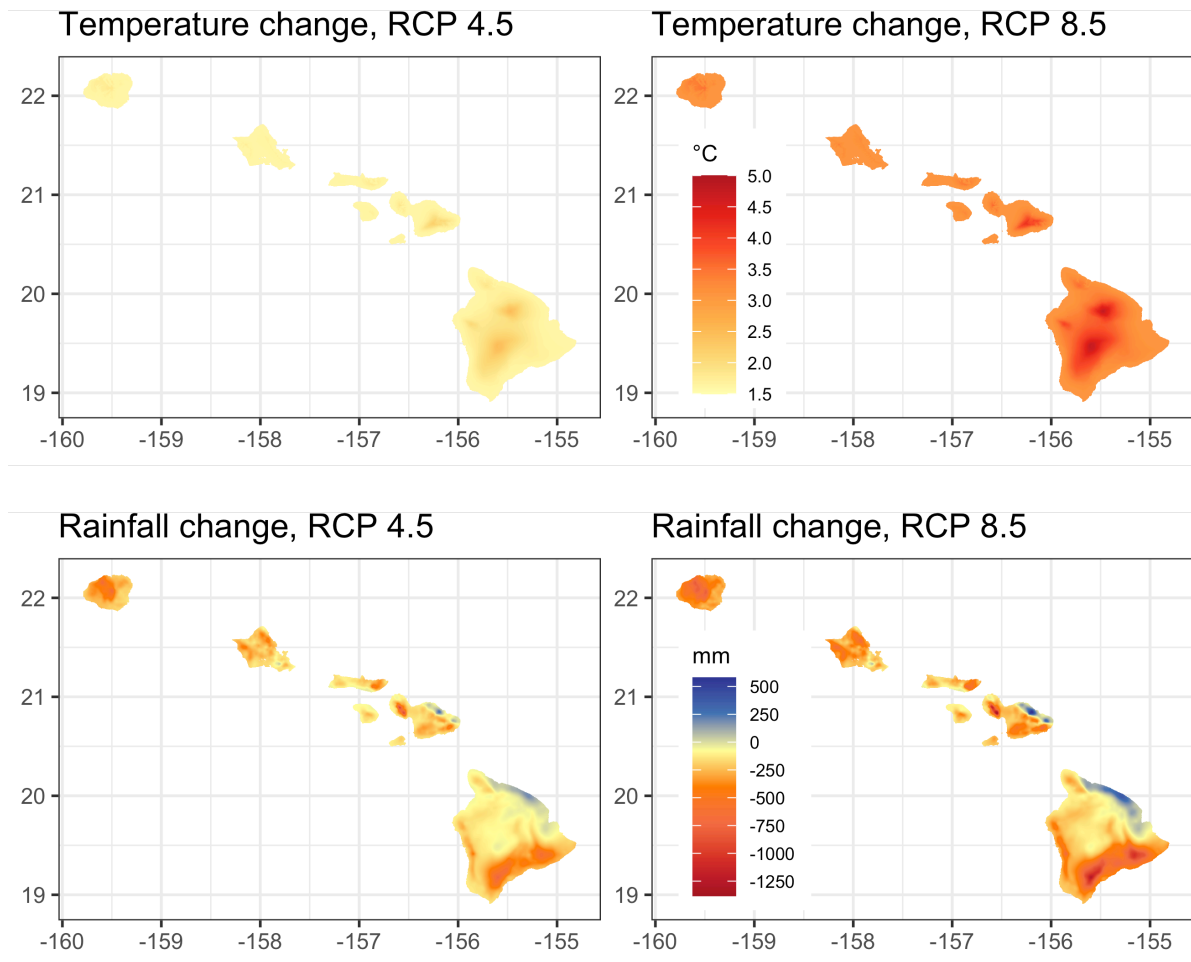


Figure 4: Supplemental - Projected change in mean annual temperature (top panels) and mean annual rainfall (bottom panels) by 2100 under RCP 4.5 and RCP 8.5 based on CMIP5 statistical downscaling. Data from *Elison Timm et al. (2015)* and *Elison Timm (2017)*.

Table 1: Supplemental - Mean IBIS-derived NPP values by Land Cover and Moisture Zone, in kg of C per square meter per year.

| Land.Cover      | NPP by Moisture Zone |       |      |
|-----------------|----------------------|-------|------|
|                 | Dry                  | Mesic | Wet  |
| Agriculture     | 0.34                 | 0.32  | 0.30 |
| Forest          | 0.29                 | 0.84  | 1.14 |
| Grassland       | 0.21                 | 0.47  | 0.81 |
| Tree Plantation | 0.29                 | 0.84  | 1.14 |
| Shrubland       | 0.31                 | 0.55  | 0.85 |
| Woody Crop      | 0.21                 | 0.67  | 0.56 |

Changes in NPP due to projected changes in climate were estimated using a set of temporal NPP multipliers representing the proportion of contemporary (2010) NPP (supplemental Figure 5) occurring in each simulation at mid-century and end-of-century under RCPs 4.5 and 8.5. We calculated temporal NPP multipliers by first estimating NPP for each simulation cell based on contemporary climate (supplemental figure 3) and projected future climates (supplemental figure 4) using empirical relationships between NPP and climate (Schuur 2003, Del Grosso *et al* 2008). We then divided contemporary NPP estimates by future NPP estimates in each simulation cell to derive mid-century and end-of-century temporal multipliers (supplemental figure 6). Annual increments were calculated by dividing mid-century and end-of-century temporal multipliers by the number of intervening years.

### ***Land Cover Change***

Projections of total land area covered by each of five land cover classes (Agriculture, Developed, Forest, Grassland and Shrubland) were summed by year and Monte Carlo iteration across the seven main Hawaiian Islands for each of two land use scenarios (low and high; supplemental Figure 7). The decline in Agricultural land between 2020 and 2040 in the low land use scenario led directly to the increase in Forest, Grassland, and Shrubland area over the same time period. Changes in agricultural land area over time in the high land use scenario reflect a balance between high rates of agricultural contraction and high rates of agricultural expansion.

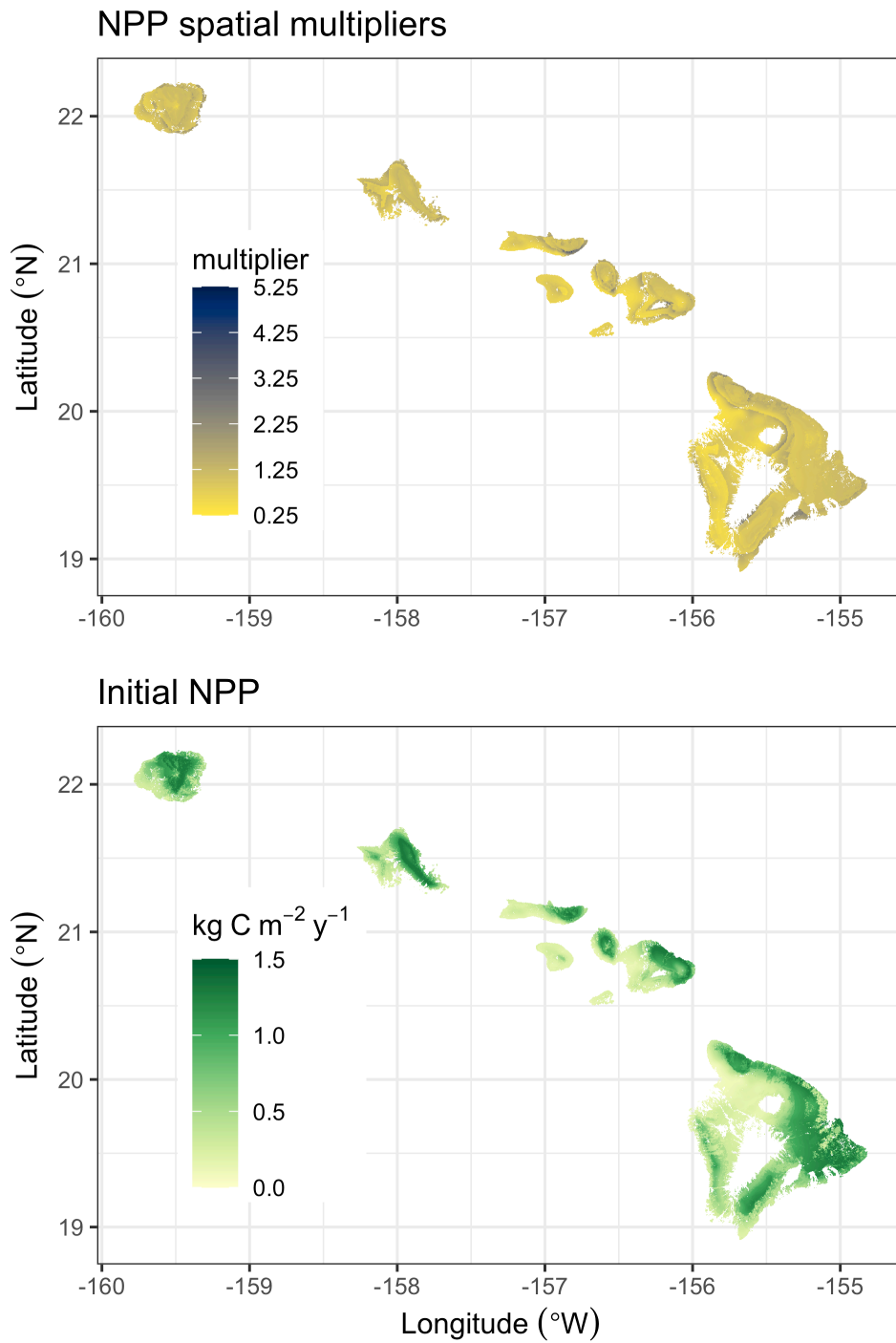


Figure 5: Supplemental - Stationary spatial NPP multipliers (top panel) and initial NPP based on the product of mean IBIS-derived NPP values (supplemental Table 1) and stationary spatial NPP multipliers (above). Developed and Barren land cover types are excluded from both maps.



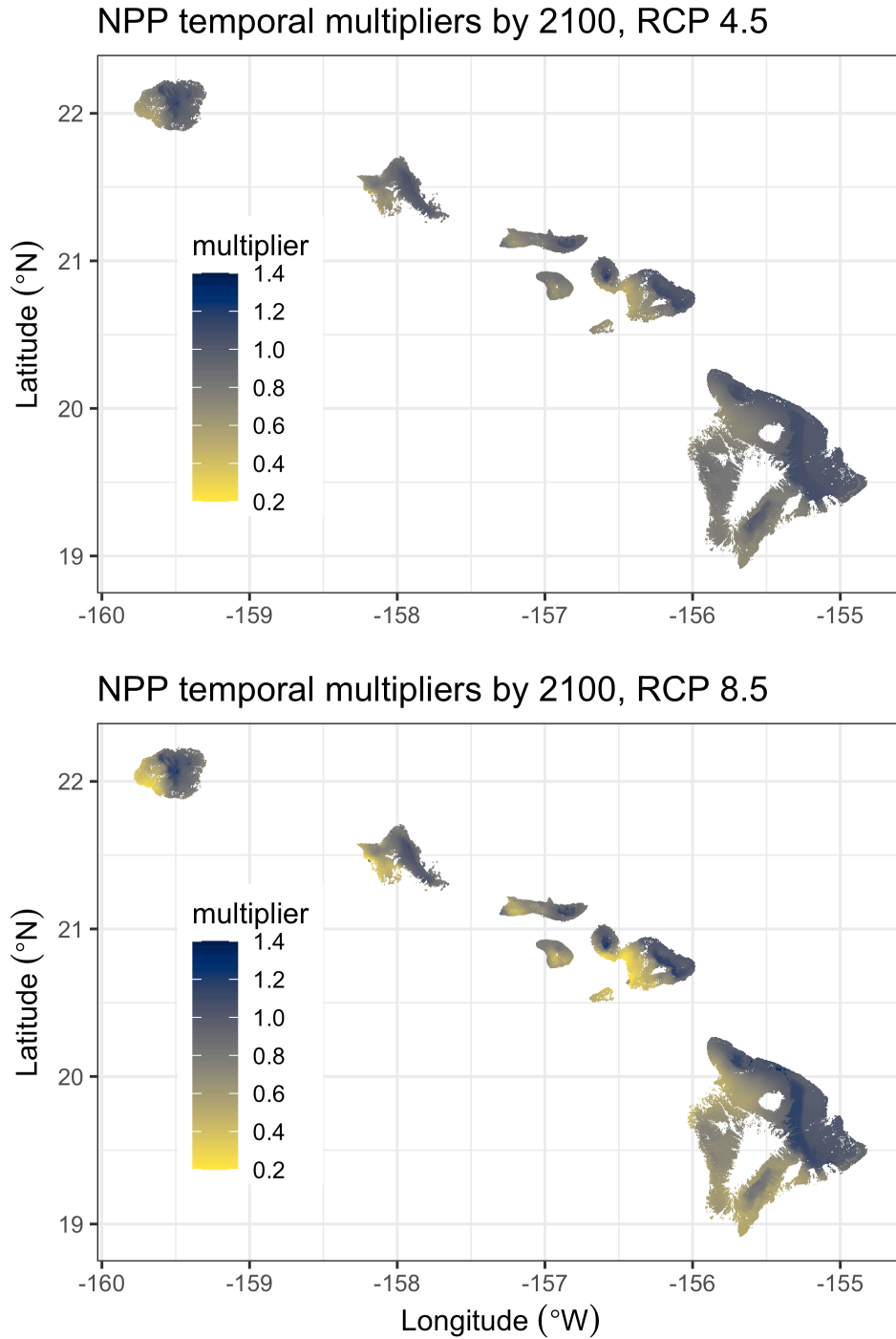


Figure 6: Supplemental - Temporal NPP multipliers for the year 2100 under RCP 4.5 (top panel) and RCP 8.5 (bottom panel). Temporal NPP multipliers represent the relative amount of initial (2010) NPP that occurs in each pixel in the year 2100 under each of two representative concentration pathways (RCPs) for atmospheric carbon dioxide. Developed and Barren land cover types are excluded from both maps.

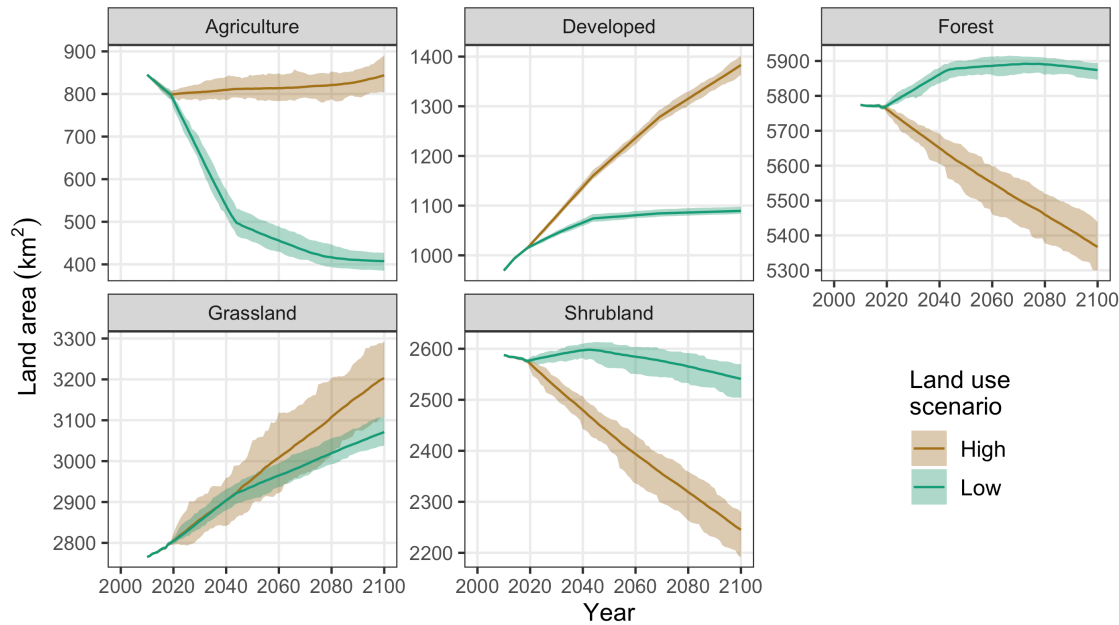


Figure 7: Supplemental - Projections of total land area by year for Agriculture, Developed, Forest, Grassland and Shrubland land cover classes in the Hawaiian Islands under low and high land use change scenarios for the period 2010-2100. Solid lines represent the mean of 30 Monte Carlo realizations and shaded areas represent minimum and maximum Monte Carlo values.

## References

- Del Grosso S, Parton W, Stohlgren T, Zheng D, Bachelet D, Prince S, Hibbard K and Olson R 2008 Global potential net primary production predicted from vegetation class, precipitation, and temperature *Ecology* **89** 2117–26
- Elison Timm O 2017 Future warming rates over the Hawaiian Islands based on elevation-dependent scaling factors *International Journal of Climatology* **37** 1093–104 Online: <https://rmets.onlinelibrary.wiley.com/doi/abs/10.1002/joc.5065>
- Elison Timm O, Giambelluca T W and Diaz H F 2015 Statistical downscaling of rainfall changes in Hawai‘i based on the CMIP5 global model projections *Journal of Geophysical Research: Atmospheres* **120** 92–112
- Giambelluca T W, Chen Q, Frazier A G, Price J P, Chen Y-L, Chu P-S, Eischeid J K and Delparte D M 2013 Online Rainfall Atlas of Hawai‘i *Bull. Amer. Meteor. Soc.* **94** 313–6

98 Giambelluca T W, Shuai X, Barnes M L, Alliss R J, Longman R J, Miura T, Chen Q, Frazier A G,  
 99 Mudd R G, Cuo L and Businger A D 2014 *Evapotranspiration of Hawai'i* Online:  
 100 <http://evapotranspiration.geography.hawaii.edu/downloads.html>  
 101 Jacobi J, Price J, Gon III S and Berkowitz P 2017 Hawaii Land Cover and Habitat Status: U.S.  
 102 Geological Survey data release Online: <https://doi.org/10.5066/F7DB80B9>  
 103 Price J, Jacobi J, Gon III S, Matsuwaki D, Mehrhoff L, Wagner W, Lucas M and Rowe B 2012  
 104 *Mapping plant species ranges in the Hawaiian Islands - developing a methodology and*  
 105 *associated GIS layers* (U.S. Geological Survey) Online: <https://pubs.usgs.gov/of/2012/1192/>  
 106 Schuur E A 2003 Productivity and global climate revisited: The sensitivity of tropical forest growth  
 107 to precipitation *Ecology* **84** 1165–70  
 108 Sleeter B M, Liu J, Daniel C, Rayfield B, Sherba J, Hawbaker T J, Zhiliang Zhu, Selmants P C and  
 109 Loveland T R 2018 Effects of contemporary land-use and land-cover change on the carbon balance of  
 110 terrestrial ecosystems in the United States *Environ. Res. Lett.* **13** 045006 Online:  
 111 <http://stacks.iop.org/1748-9326/13/i=4/a=045006>  
 112 Sleeter B M, Marvin D C, Cameron D R, Selmants P C, Westerling A L, Kreitler J, Daniel C J, Liu J  
 113 and Wilson T S 2019 Effects of 21st-century climate, land use, and disturbances on ecosystem carbon  
 114 balance in California *Global Change Biology* **25** 3334–53